Although each organization recommends a variety of measurement protocols and frequencies, as shown in Table 1, our data suggest that the sensitivity, which changed at a rate of roughly 5% per year, should be examined more than twice a year at least for an SET2400W scanner. The spatial resolution should be monitored once a year; this is considered sufficient as the spatial resolution showed only a slight change with aging. Our previous observation using a PT931/04 scanner (block detector) also indicated that the spatial resolution was stable, whereas the sensitivity was reduced by approximately 30% during the 13 years after installation [6]. This result also indicates that the sensitivity tends to be more severely affected by aging than the spatial resolution even for other block-detector-type PET scanners. It is assumed that a spatial resolution should be measured less frequently than sensitivity for the block-detector-type scanner. Finally, the random fraction, which displayed smaller variations than the sensitivity, needs to be measured more than once a year for our PET scanner.

In summary, the results have indicated that this scanner can sustain a proper performance level for more than 10 years when maintained in an appropriate manner. Indeed, periodic monitoring is necessary for detecting early performance deterioration. Regarding our scanner, the largest variation (deterioration) was observed in sensitivity compared with other parameters. The reduction in sensitivity can be calculated easily from CCF measurement data, which is measured routinely at every institute. Therefore, CCF measurement is an easy and useful method for monitoring and maintaining the performance of PET scanners against aging. As the present data were obtained from a single scanner, the authors encourage the initiation of a follow-up study involving various scanners.

Acknowledgments The authors thank Mr. Kazumi Tanaka (Shimadzu Co. Ltd.) for giving us valuable information and comments.

References

1. Jhanwar YS, Straus DJ. The role of PET in lymphoma. J Nucl Med. 2006;47(8):1326–34.
2. Herholz K, Carter SF, Jones M. Positron emission tomography imaging in dementia. Br J Radiol. 2007;80 Spec No 2:S160–7.
3. Knuuti J, Schelbert HR, Bax JJ. The need for standardisation of cardiac FDG PET imaging in the evaluation of myocardial viability in patients with chronic ischaemic left ventricular dysfunction. Eur J Nucl Med Mol Imaging. 2002;29(9):1257–66.
4. Cook GJ. Pitfalls in PET/CT interpretation. Q J Nucl Med Mol Imaging. 2007;51(3):235–43.
5. Halldin C, Gulyas B, Langer O, Farde L. Brain radioligands-state of the art and new trends. Q J Nucl Med. 2001;45(2):139–52.
6. Watanuki S, Ishii K, Itoh M, Orihara H. Reliability of a positron emission tomography system (CTI:PT931/04-12). Kaku Igaku. 2002;39(2):155–60.
7. International Electrotechnical Commission. Part 1. Positron emission tomographs. In: International, Electrotechnical, and Commission, editors. IEC Standard 61675-1: radionuclide imaging devices—characteristics and test conditions. Geneva: International Electrotechnical Commission; 1998.
8. American College of Radiology. ACR technical standard for medical nuclear physics performance monitoring of PET-CT imaging equipment. Reston: American College of Radiology; 2006.
9. Japan Industries Association of Radiological Systems. Standard for maintenance of positron emission tomographs. JESRA TI-0001-1994; 1994.
10. Fujiwara T, Watanuki S, Yamamoto S, Miyake M, Seo S, Itoh M, Ishii K, Orihara H, Fukuda H, Satoh T, Kitamura K, Tanaka K, Takahashi S. Performance evaluation of a large axial field-of-view PET scanner: SET-2400 W. Ann Nucl Med. 1997;11(4):307–13.
11. Bettinardi V, Danna M, Savi A, Lecchi M, Castiglioni I, Gilardi MC, Bammer H, Lucignani G, Fazio F. Performance evaluation of the new whole-body PET/CT scanner: Discovery ST. Eur J Nucl Med Mol Imaging. 2004;31(6):867–81.
12. Erdi YE, Nehmeh SA, Mulnix T, Humm JL, Watson CC. PET performance measurements for an LSO-based combined PET/CT scanner using the National Electrical Manufacturers Association NU 2–2001 standard. J Nucl Med. 2004;45(5):813–21.
13. Reist HW, Stadelmann O, Kleeb W. Study on the stability of the calibration and normalization in PET and the influence of drifts on the accuracy of quantification. Eur J Nucl Med. 1989;15(11):732–5.
14. Spinks T, Jones T, Heather J, Gilardi M. Quality control procedures in positron tomography. Eur J Nucl Med. 1989;15(11):736–40.
15. Matsumoto K, Yamamoto S, Wada Y, Shimizu K, Murase K, Senda M. Reliability of plural measuring instruments for quantitative PET measurement -performance of dose-calibrator, auto well gamma counter, continuous blood sampling system, and PET scanner. Nippon Hoshasen Gijutsu Gakkai Zasshi. 2008;64(10):1227–34.
16. Zhang H, Alyafei S, Inoue T, Tomiyoshi K, Endo K. Performance stability of SHR-2000 high resolution PET for animal research. Ann Nucl Med. 1999;13(1):65–70.
17. National Electrical Manufacturers Association. NEMA standards publication NU 2-1994 performance measurements of positron emission tomographs. Rosslyn: National Electrical Manufacturers Association; 1994.
18. National Electrical Manufacturers Association. NEMA standards publication NU 2-2001: performance measurements of positron emission tomographs. Rosslyn: National Electrical Manufacturers Association; 2001.
19. Uribe J, Li H, Baghaei H, Aykac M, Wang Y, Liu Y, Xing T, Wong WH. Effect of photomultiplier gain-drift and radiation exposure on 2D-map decoding of detector arrays used in positron emission tomography. IEEE Nucl Sci Symp Med Imaging Conf. 2001;4:1960–4.
20. Melcher CL. Scintillators for Well Logging Applications. Nuclear Inst. and Methods in Physics Research. 1989;(B40-41):1214–8.
21. Belakhlef S, Church C, Hays A, Fraser R, Lakhanpal S. Quantitative assessment of the influence of location, internal temperature, idle time, and normalization on the sensitivity of a mobile PET/CT scanner. J Nucl Med Technol. 2008;36(3):147–50.
22. Williams JJ, McDaniel DL, Kim CL, West LJ. Detector characterization of discovery ST whole-body PET scanner. IEEE Nucl Sci Symp Conf Rec. 2003;2:717–21.
23. Japan Industries Association of Radiological Systems. Performance measurement of positron emission tomographs; JESRA X-0073*A-2005. Japan Industries Association of Radiological Systems; 2005.

Progression from Unilateral to Bilateral Parkinsonism in Early Parkinson Disease: Implication of Mesocortical Dopamine Dysfunction by PET

Shunsuke Yagi[1], Etsuji Yoshikawa[2], Masami Futatsubashi[2], Masamichi Yokokura[3], Yujiro Yoshihara[3], Tatsuo Torizuka[4], and Yasuomi Ouchi[1]

[1]Molecular Imaging Frontier Research Center, Hamamatsu University School of Medicine, Hamamatsu, Japan; [2]Central Research Laboratory, Hamamatsu Photonics K.K., Hamamatsu, Japan; [3]Department of Psychiatry and Neurology, Hamamatsu University School of Medicine, Hamamatsu, Japan; and [4]Research Center for Child Mental Development, Hamamatsu University School of Medicine, Hamamatsu, Japan

It is still unclear why some early Parkinson disease (PD) patients with unilateral parkinsonism develop bilateral parkinsonism soon after the diagnosis is made as Hoehn and Yahr (HY) stage 1 and others remain stable for a long time. Here, we examined in vivo changes in the brain dopaminergic system using PET with a dopamine transporter radiotracer, ^{11}C-2-B-carbomethoxy-3B-(4-fluorophenyl) tropane (^{11}C-CFT), to elucidate the pathophysiologic characteristics of the dopamine system in early converters. **Methods:** Twelve drug-naïve PD patients with HY stage 1 disease and 8 age-matched healthy subjects participated in this study. Clinical evaluation of their parkinsonism was performed monthly until their HY stage 1 (unilateral parkinsonism) disease had become stage 2 (bilateral parkinsonism) disease according to the Unified Parkinson Disease Rating Scale. The endpoint of the follow-up study was the time of the conversion. Region-of-interest analysis was used to examine ^{11}C-CFT binding in the mesocortical (nucleus accumbens, caudate, orbitofrontal cortex) and nigrostriatal (putamen) dopamine projection regions. Multiregression analyses between these PET data and clinical parameters were performed within the PD group. **Results:** Between-group comparisons showed that, irrespective of the duration of conversion, all PD patients clinically diagnosed at HY stage 1 had a significant reduction in ^{11}C-CFT binding in the bilateral striatum (affected, −46%; unaffected, −35%). Regression analysis showed that the level of ^{11}C-CFT binding in the nucleus accumbens and orbitofrontal cortex on the unaffected side was significantly positively correlated with the conversion interval. This positive correlation indicates that the more severe a dysfunction presents in the mesocortical dopamine system on the seemingly intact side, the more rapidly the parkinsonism proceeds to the intact side (bilateral parkinsonism). **Conclusion:** The finding of bilateral reduction in the striatal ^{11}C-CFT binding even in HY stage 1 PD patients confirms that molecular changes in the dopamine system precede clinical phenotype, suggesting an advantage of PET for detecting an early abnormality of the disease. The spread of parkinsonism to the unaffected side soon after the diagnosis of HY stage 1 PD may be related to the degree of mesocortical dopamine dysfunction.

Key Words: ^{11}C-CFT; mesocortical dopamine function; unilateral parkinsonism; Parkinson disease; positron emission tomography

J Nucl Med 2010; 51:1250–1257
DOI: 10.2967/jnumed.110.076802

The diagnosis of Parkinson disease (PD) is based on clinical assessment, which is also used to evaluate disease progression before therapeutic intervention. The neuropathologic process involved in PD is loss of the nigral dopamine neurons and the ensuing loss of dopamine nerve terminals in the striatum (*1,2*). Although the extent of the annual reduction in dopamine neurons is estimated to be around 10% (*3,4*), the exact rate of disease progression varies from patient to patient. This variation makes decisions on medication difficult in the clinical setting because administering the normal doses of levodopa and other antiparkinsonian drugs irrespective of the severity of parkinsonian symptoms would not always be appropriate. We previously reported that even in early-stage PD, dopamine dysfunction is present not only in the striatal but also in the mesocortical dopaminergic projection system and that mesocortical dysfunction might contribute to mental and behavioral impairment (*5*). Our findings indicate that the level of dopamine function in the mesocortical system may be a key surrogate marker of the progression of PD.

Many in vivo studies have used PET with several radiotracers for presynaptically located dopamine transporters to

Received Mar. 1, 2010; revision accepted Apr. 28, 2010.
For correspondence or reprints contact: Yasuomi Ouchi, Molecular Imaging Frontier Research Center, Hamamatsu University School of Medicine, 1-20-1 Handayama, Higashi-ku, Hamamatsu 431-3192, Japan.
E-mail: ouchi@hama-med.ac.jp

match PET findings with pathology in the postmortem PD brain (*6,7*). The advantage of using PET is its ability to depict functional abnormalities in dopamine neurons at the molecular level before clinical phenotypes appear. For example, motor symptoms do not develop until 50%–60% of dopamine neurons (binding of tracers) have been affected (*8,9*). Although PET of the dopamine transporter cannot differentiate the number of dopamine transporters per synapse from the number of dopamine terminals in PD, imaging of the dopamine transporter is of diagnostic value because reduction in dopamine transporter comes earlier than changes in dopamine content in the PD-model monkeys (*10*). Therefore, this technique allows us to predict the progression of the disease by examining the vulnerability of dopamine neurons at the molecular level.

The purpose of the present study was to compare the binding level of ^{11}C-2-B-carbomethoxy-3B-(4-fluorophenyl) tropane (^{11}C-CFT, a marker for the membrane dopamine transporter) in dopaminergic projection (mesocortical and nigrostriatal) regions at an early stage of PD (Hoehn and Yahr [HY] stage 1) with the interval of conversion from HY stage 1 to HY stage 2 to clarify whether dopamine abnormalities in any brain region can act as a surrogate marker of the clinical progression of early-stage PD.

MATERIALS AND METHODS

Participants

We studied 12 drug-naïve patients with HY stage 1 PD (5 men, 7 women; mean age ± SD, 58.8 ± 9.3 y) and 8 healthy subjects (5 men, 3 women; mean age ± SD, 51 ± 15.5 y). We obtained their written informed consent for the present study, which was also approved by the local ethics committee of Hamamatsu Medical Center. Each PD patient was clinically assessed using the Unified Parkinson Disease Rating Scale (UPDRS). Patients who had limb tremors, rigidity, and bradykinesia and who had received a tentative clinical diagnosis of PD were recruited from our main hospital or the neighboring clinics. Controls who were physically healthy and did not have or were not being treated for any neurologic complications were recruited by in-house advertisement. All participants underwent MRI, a neuropsychiatric examination, and a blood test to exclude the possibility of any accompanying disease. None of the participants had major depression, dementia, or a history of psychostimulant drug abuse. The UPDRS evaluation was performed just before the PET examination. The UPDRS scores varied from 11 to 25. The duration of disease was from 4 to 33 mo (mean, 16.2 mo). The disease duration was defined by the time from initial symptoms. Because all PD patients were diagnosed as having a clinical severity of HY stage 1, their limbs were affected unilaterally (left-sided in 4 patients and right-sided in 8 patients). More detailed clinical characteristics of the patients are listed in Table 1.

MRI and PET

Before the PET scan, MRI (0.3-T MRP7000AD; Hitachi) was performed with 3-dimensional mode sampling (repetition time/echo time, 200/23; flip angle, 75°; slice thickness, 2 mm, with no gap; matrices, 256 × 256). Each piece of MRI data was used to determine suitable areas for region-of-interest (ROI) analysis. With the aid of data relating to tilt angle and spatial coordinates obtained during the procedure for determining the intercommisural (anterior commissure–posterior commissure [AC-PC]) line on each subject's sagittal MR images, a PET gantry was set parallel to the AC-PC line by tilting and moving the gantry for each study. This set-up enabled us to reconstruct the PET images parallel to the AC-PC line, without reslicing (*11*).

The details of the PET procedure are given elsewhere (*5,12*). In brief, we used a high-resolution brain PET scanner with 24 detector rings yielding 47 slice images simultaneously (SHR12000; Hamamatsu Photonics KK). After head-fixation using a thermoplastic face mask and a 10-min transmission scan for attenuation correction, serial scans (time frames, 4 × 30, 20 × 60, and 14 × 300 s) were

TABLE 1. Characteristics of PD Patients

Patient no.	Sex	Age (y)	Duration of illness (mo)*	UPDRS total	Affected side	Initial symptom
1	F	44	18	11 (2/3/6)	L	Rigidity
2	F	55	12	13 (2/3/8)	L	Rigidity/tremor (UL/LL)
3	M	67	14	14 (1/2/11)	R	Tremor (UL)
4	F	60	24	16 (2/3/11)	R	Tremor (UL/LL)
5	M	58	25	16 (4/6/6)	R	Rigidity/tremor (UL)
6	F	58	10	17 (2/5/10)	R	Rigidity/tremor (UL)
7	F	71	9	18 (2/4/12)	R	Rigidity/tremor (UL)
8	M	56	33	18 (4/4/10)	R	Rigidity/tremor (UL/LL)
9	F	73	4	20 (2/2/16)	L	Rigidity/tremor (UL/LL)
10	M	64	6	21 (2/4/15)	R	Rigidity
11	M	43	12	21 (2/6/13)	L	Rigidity/tremor (UL)
12	F	57	28	25 (4/5/16)	R	Rigidity/tremor (UL)

*Duration between disease onset and PET examination.
UPDRS scores in parentheses are mentation/activities of daily living/motor examination.
UL = upper limb; LL = lower limb.

obtained for 92 min after a slow bolus venous injection of a 6 MBq/kg dose of ^{11}C-CFT. Arterial blood sampling was not performed in the present study.

Image Data Processing

Irregular ROIs were located bilaterally on the nucleus accumbens, nucleus caudate, ventral putamen, dorsal putamen, orbitofrontal cortex, and cerebellum (Fig. 1) on the MR images (*13*). The ROIs were then automatically transferred onto the corresponding ^{11}C-CFT distribution images (reconstructed from 70 to 90 min after the tracer injection) using image-processing software (Dr View; Asahi Kasei Co.) on a workstation (Hypersparc ss-20; SUN Microsystems) (*5*). We calculated the reference tissue–derived ratio index (RI) (i.e., the ratio of the PET count in the target region to the PET count in the cerebellum in the late integrated image) because the value of this ratio reflects the binding potential estimated by the quantitative 3-compartment 4-parameter model for ^{11}C-CFT, which we tested previously (*14*). The PET image used for the ROI setting comprised 2 consecutive images that covered slices (thickness, 6.8 mm) in the z direction (*15*), so each ROI value contained functional information about the striatum to a depth of at least 6.8 mm in the z direction (volume data).

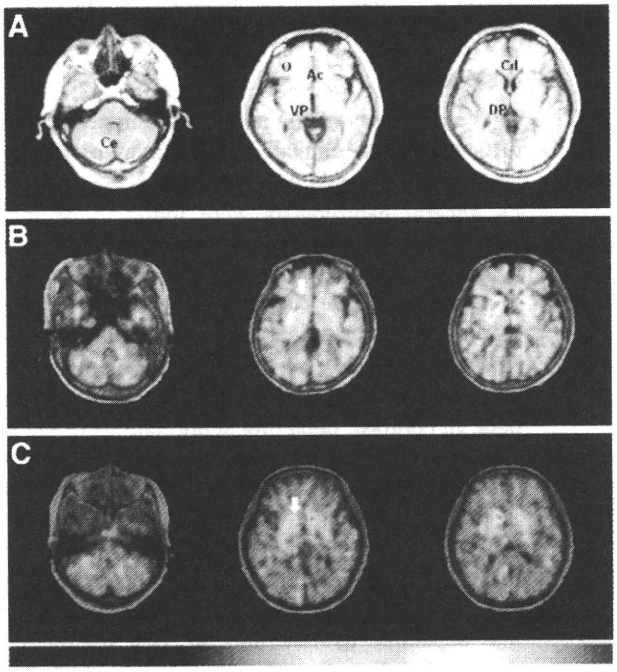

FIGURE 1. ^{11}C-CFT PET images and ROI setting. (A) Irregular ROIs, drawn bilaterally on concerned regions on MR images, were placed on corresponding PET images. (B) PD patient with longer conversion period from HY stage 1 to HY stage 2. (C) PD patient with shorter conversion period from HY stage 1 to HY stage 2. Arrow indicates reduction in ^{11}C-CFT binding in nucleus accumbens. Color bar indicates quantified level of RI (from 0 to 3). Ac = nucleus accumbens; Cd = caudate; Ce = cerebellum; DP = dorsal putamen; O = orbitofrontal cortex; VP = ventral putamen.

Statistics

Student t tests were conducted to compare all estimates in the brain regions between the PD and control groups. A P value of less than 0.05 was considered to be statistically significant. Although an age-related reduction in ^{11}C-CFT binding was reported (*16*), we compared the estimates without age correction because there was no difference in age between the 2 groups. Pearson regression coefficient analysis was performed for comparisons between ^{11}C-CFT RI values and the patients' clinical variables. To examine dopamine projection regions in which alterations in ^{11}C-CFT binding might be linked to disease prognosis, multiple regression analyses were performed between the regional ^{11}C-CFT levels at HY stage 1 and the duration required for the conversion from HY stage 1 to HY stage 2. A P level of less than 0.05 after Bonferroni adjustment was used to indicate statistical significance.

RESULTS

Level of ^{11}C-CFT Binding in HY Stage 1 PD

Compared with the values in their healthy counterparts (Table 2), ^{11}C-CFT RI values in the PD patients were significantly reduced not only on the affected side but also on the unaffected side. The following were the reduced values in the different regions: ventral putamen, 50% on the affected side versus 39% on the unaffected side; dorsal putamen, 61% on the affected side versus 45% on the unaffected side; nucleus accumbens, 38% on the affected side versus 32% on the unaffected side; caudate, 34% on the affected side versus 22% on the unaffected side; and orbitofrontal cortex, 34% on the affected side versus 28% on the unaffected side.

Correlation Between ^{11}C-CFT Binding and Clinical Variables at HY Stage 1

Statistics with Bonferroni adjustment showed that all regression results fell outside the statistically significant limit (Fig. 2) ($P > 0.05$, corrected for multiple comparison). The ^{11}C-CFT RI values in each brain region tended to be negatively correlated with the UPDRS scores: nucleus accumbens (affected: $r = -0.408$; unaffected: $r = -0.787$), caudate (affected: $r = -0.709$; unaffected: $r = -0.703$; $P > 0.05$ corrected), orbitofrontal cortex (affected: $r = -0.404$; unaffected: $r = -0.58$); ventral putamen (affected: $r = -0.603$; unaffected: $r = -0.455$); dorsal putamen (affected: $r = -0.682$; unaffected: $r = -0.564$). There was also a tendency toward a negative correlation between the UPDRS subscores and the ^{11}C-CFT RI values (not shown).

Association of Initial ^{11}C-CFT Binding with Clinical Progression

As shown in Table 3, all PD patients were treated with antiparkinsonian drugs, among which levodopa was

TABLE 2. Levels of ^{11}C-CFT Uptake in PD Patients and Controls

Subject	Nucleus accumbens		Caudate		Putamen				Orbitofrontal	
					Ventral		Dorsal			
	Affected side	Unaffected side	Affected side	Unaffected side	Affected side	Unaffected side	Affected side	Unaffected side	Affected side	Unaffected side
Healthy control (n = 8)	2.08 ± 0.20		2.23 ± 0.24		2.36 ± 0.29		2.51 ± 0.33		0.25 ± 0.08	
PD patient (n = 12)	1.29 ± 0.30	1.42 ± 0.25	1.48 ± 0.38	1.75 ± 0.30	1.18 ± 0.36	1.43 ± 0.37	0.99 ± 0.35	1.40 ± 0.47	0.17 ± 0.04	0.18 ± 0.06
% reduction	38%	32%	34%	22%	50%	39%	61%	45%	34%	28%

Each value is expressed as ratio index. % reduction denotes level of change in ratio index of PD patient compared with healthy control.

prescribed to all patients. Only 1 patient who had undergone a PET examination dropped out, because of a family issue. The mean duration required for conversion from HY stage 1 to stage 2 was 2.9 ± 1.5 y and ranged from 6 mo to 5 y in the PD group. No specific relevance was found between the conversion interval and the kinds of antiparkinsonian drugs administered, and the doses of each drug varied mildly among the patients.

Regression analyses with Bonferroni adjustment showed that the initial values of ^{11}C-CFT RI in the nucleus accumbens, caudate, and orbitofrontal cortex on the unaffected side were significantly positively correlated with the conversion interval (nucleus accumbens, affected: $r = 0.628$, $P > 0.05$, unaffected: $r = 0.889$, $P < 0.05$ corrected; caudate, affected: $r = 0.709$, $P > 0.05$, unaffected: $r = 0.866$, $P < 0.05$ corrected; and orbitofrontal cortex, affected: $r = 0.682$, $P > 0.05$, unaffected: $r = 0.735$, $P < 0.05$ corrected) (Fig. 3). In other words, dopamine hypofunction in the mesocortical dopamine system contralateral to the affected limb likely indicates rapid progression to bilateral parkinsonism. There was a tendency toward a positive correlation in these regions on the affected side (ventral putamen, affected: $r = 0.695$, unaffected: $r = 0.685$; dorsal putamen, affected: $r = 0.510$, unaffected: $r = 0.689$).

DISCUSSION

The diagnosis of PD and determining its prognosis are difficult in the clinical setting, as shown by previous studies that reported that the initial diagnoses of PD made by general neurologists were found to be incorrect at autopsy in 24%–35% of cases (*17,18*). In addition, around 8.1% of the patients diagnosed with PD were later found to have an alternate diagnosis based on multifactorial clinical diagnostic criteria after a mean follow-up of 6 y (*19*). These reports indicate the difficulty of making a precise evaluation of possible PD cases based solely on clinical data. In contrast, depicting abnormalities of the dopamine system on a molecular basis has a greater advantage (*6,20–25*). Previous studies showed that the progression of PD was associated with a similar rate of dopaminergic losses in all striatal subregions (*26*). In line with the results of previous studies, our findings (initial dopaminergic loss in the posterodorsal striatum and the following mesocortical dopamine dysfunction) are best interpreted as evidence of colinearity of degeneration, with progression across striatal regions. In other words, patients with initially more significant denervation (yet clinically still in HY stage 1) were likely to reach the conversion point sooner than were stage 1 patients with less severe denervation. This might be true because the correlation coefficients across the striatal subregions all showed an r value greater than 0.5. The higher levels of statistical significance for the anterior striatal regions is better explained by relative floor denervation effects in the more posterior regions (*27*).

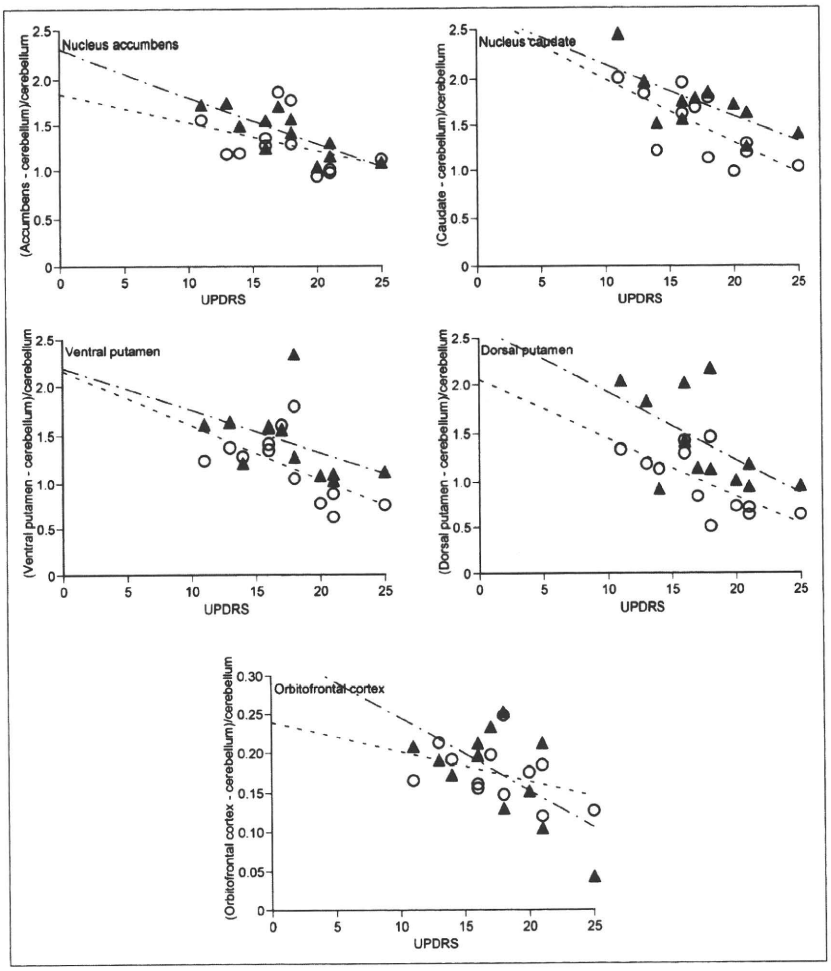

FIGURE 2. Correlations between UPDRS score at HY stage 1 and ^{11}C-CFT RI values. Dashed lines for ○ and chain lines for ▲ show all tendencies of negative correlations. ○ = affected side; ▲ = unaffected side.

In all patients with HY stage 1 PD, a significant reduction in ^{11}C-CFT binding was found in the dorsal putamen, which was in line with the previous findings from early PD patients with HY stage 1 or stage 2 disease (*6*). This reduction is also consistent with pathologic evidence showing the most severe neuronal loss in the ventrolateral part of the substantia nigra, which projects mainly to the posterior putamen (*9,28*). However, this regional

TABLE 3. Details of PD Patients at Time of Progression to HY Stage 2

Patient no.	Interval (y)*	% Increase of UPDRS†	Levodopa (mg/d)	Dopamine agonist (mg/d)	Anticholinergic agent (mg/d)	Selegiline (mg/d)
1	5	73	200	0.5	4	—
2	5	100	100	0.5	4	—
3	2	71	200	0.75	4	5
4	3	38	100	0.5	4	—
5	1.8	75	200	0.75	4	5
6	4	65	100	0.5	4	—
7	4.4	33	100	0.5	4	—
8	3	33	100	0.5	4	—
9	2	40	100	0.5	4	—
10	—	—	—	—	—	—
11	1.5	48	200	0.75	4	5
12	0.5	44	200	0.75	4	5

*Interval of conversion from HY stage 1 to stage 2.
†% increase of UPDRS = [UPDRS at HY stage 2 ("on" state) − initial UPDRS at HY stage 1]/initial UPDRS at HY stage 1 × 100.
No information was available for patient 10 because patient dropped out of study.

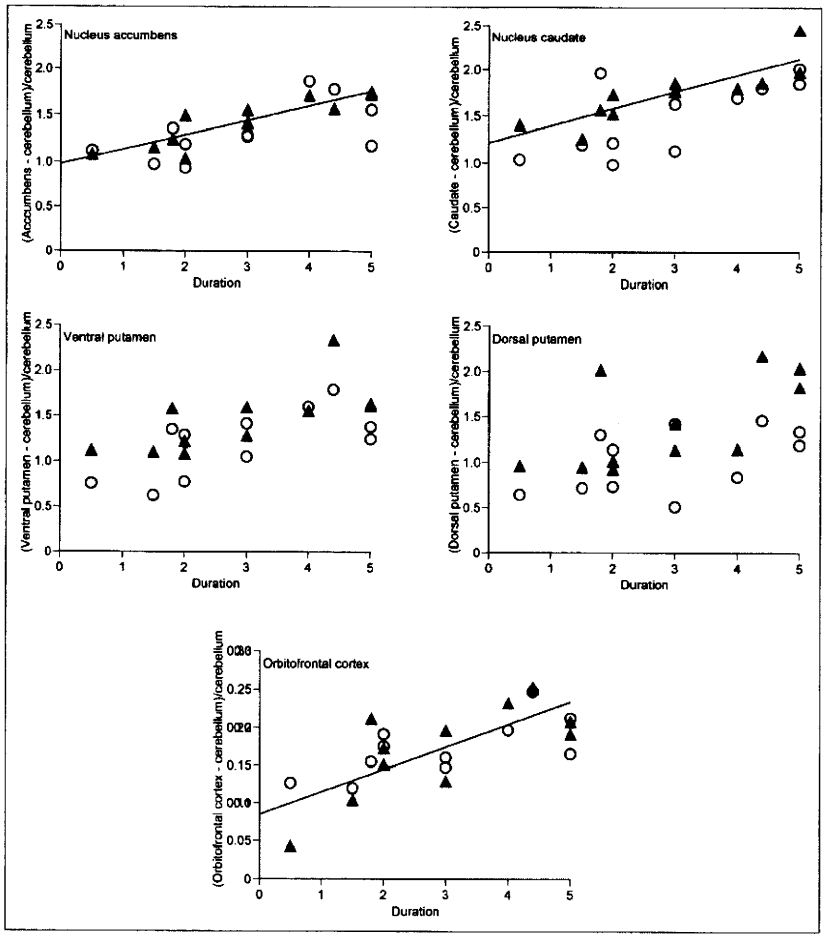

FIGURE 3. Correlations between conversion interval (y) and ^{11}C-CFT RI values. Straight lines for ▲ show significant correlations ($P < 0.05$). ○ = affected side; ▲ = unaffected side.

vulnerability does not always result in an orderly progression of parkinsonism—that is, a prolonged period at HY stage 1 or quick conversion from stage 1 to stage 2, and such, in the clinical setting. In our study, we examined the correlation between the clinical progression of PD (HY stage 1 to stage 2) and regional ^{11}C-CFT binding. As a result, we found that the reduction of ^{11}C-CFT binding in the dorsal putamen did not correlate significantly with conversion time (progression), irrespective of its laterality. In contrast, ^{11}C-CFT binding in the nucleus accumbens, caudate, and orbitofrontal cortex on the unaffected side was significantly positively associated with conversion time, suggesting that mesocortical dopamine function determines the prognosis of the disease. ^{11}C-CFT binding in the mesocortical dopamine region did not correlate with symptomatic deterioration (data not shown). Rather, nigrostriatal dysfunction may reflect a symptomatologic change in PD, as reported elsewhere (*29*). Thus, mesocortical involvement may be an important predictor of the progression of PD from unilateral to bilateral parkinsonism. This in vivo finding is of biologic value because there is no clear consensus on whether the Braak pathologic progression theory (*30*) of PD has any clinical relevance (*31*).

Although all patients examined in the present study were diagnosed with unilateral parkinsonism (HY stage 1), striatal ^{11}C-CFT binding was already significantly lower, even on the side ipsilateral to the affected limb. This observation was in line with a previous finding from a ^{123}I-β-CIT SPECT study (*32*), supporting the authors' conclusion that imaging of dopamine tracer binding might serve as a tool for identifying individuals developing dopaminergic pathologic conditions before the onset of motor symptoms. Lateralization of parkinsonian symptoms with bilateral biotracer reduction in the striatum may be a common phenomenon at the time when patients first consult a doctor. There is no clear explanation as to why mesocortical dysfunction on the unaffected side leads to bilateral parkinsonism. One possibility is that any damage of the extrastriatal cortical region, especially the mesocortical projection region, would enhance latent further losses of putaminal dopamine transporter, which cause clinical manifestation of parkinsonism. Psychophysiologically, a dysfunction in the mesocortical dopamine system—which mediates affect, behavior, and cognition (*33*)—would negatively affect the nigrostriatal system through mutual neural interactions (*34*). Methodologically, however, one caveat is a low den-

sity of dopamine transporter outside the striatal region (*35*). Despite this, the presence of different values in the orbitofrontal cortex could reflect a minor but significant alteration in PD pathophysiology.

In the present study, there was no marked difference in the medication administered during the course of the disease because the treatment of all patients was based on a standardized algorithm (*36,37*). As a result, we could not clarify the differences between various treatment regimens. Although the dose of levodopa is similar among the patients in the current study, there would be a possibility that levodopa treatment might affect the parkinsonism progression. Because it has been recently reported that levodopa significantly affects the corticoputaminal loop but does not affect the corticocaudatal loop as much (*38*), the treatment might not be a significant confounding factor in the present result on the mesocortical system. Regarding antiparkinsonian drugs, there are reports that the progressive reduction in dopamine transporter binding was smaller during agonist-based therapy than in levodopa-based therapy (*39*) and that the mean improvement in total, motor, and ADL UPDRS scores was greater in the levodopa group. Antiparkinsonian drugs are considered to have some neuroprotective efficacy, but no established evidence by neuroimaging techniques has been reported in a clinical setting (*40*). Taken together, on the basis of our results, a cognitive stimulator that acts on the mesocortical dopamine system might be a promising drug treatment for HY stage 1 PD patients.

CONCLUSION

Because drug-naïve PD patients with unilateral parkinsonism diagnosed as HY stage 1 showed significantly lower levels of ^{11}C-CFT binding in the bilateral striatum in the present study, it is clear that molecule-based dopamine functional alterations in the brain precede the PD phenotype. The progression of parkinsonism may possibly be related to additional dysfunction of the mesocortical dopamine system, although this dysfunction is of little use for predicting deterioration in extrapyramidal symptoms. Thus, molecular imaging with ^{11}C-CFT is a useful method for assessing the pathophysiology of PD and its progression. Still, the mechanism of the development of PD remains unclear, as does the relevance of mesocortical neuronal damage to PD progression. Further, human-based imaging studies using other neurotransmitter tracers or a new tracer specific to the disease entity such as synuclein are needed.

ACKNOWLEDGMENTS

We thank Dr. Masanobu Sakamoto and Toshihiko Kanno and Yasuo Tanizaki (Hamamatsu Medical Center), Yutaka Naito (Japan Environment Research Corporation), and Akihito Oda (Hamamatsu Photonics KK) for their support. This work was supported by a Research Grant for Longevity Science from the Ministry of Health, Labor and Welfare, Japan, and a grant from the Takeda Science Foundation.

REFERENCES

1. German DC, Manaye K, Smith W, Woodward D, Saper C. Midbrain dopaminergic cell loss in Parkinson's disease: computer visualization. *Ann Neurol.* 1989;26:507–514.
2. McGeer PL, Itagaki S, Akiyama H, McGeer E. Rate of cell death in parkinsonism indicates active neuropathological process. *Ann Neurol.* 1988;24: 574–576.
3. Marek K, Innis R, van Dyck C, et al. [^{123}I]β-CIT SPECT imaging assessment of the rate of Parkinson's disease progression. *Neurology.* 2001;57:2089–2094.
4. Hilker R, Schweitzer K, Coburger S, et al. Nonlinear progression of Parkinson disease as determined by serial positron emission tomographic imaging of striatal fluorodopa F18 activity. *Arch Neurol.* 2005;62:378–382.
5. Ouchi Y, Yoshikawa E, Okada H, et al. Alterations in binding site density of dopamine transporter in the striatum, orbitofrontal cortex, and amygdala in early Parkinson's disease: compartment analysis for β-CFT binding with positron emission tomography. *Ann Neurol.* 1999;45:601–610.
6. Frost JJ, Rosier A, Reich S, et al. Positron emission tomographic imaging of the dopamine transporter with ^{11}C-WIN 35,428 reveals marked declines in mild Parkinson's disease. *Ann Neurol.* 1993;34:423–431.
7. Frey KA, Koeppe R, Kilbourn M, et al. Presynaptic monoaminergic vesicles in Parkinson's disease and normal aging. *Ann Neurol.* 1996;40:873–884.
8. Fearnley JM, Lees AJ. Ageing and Parkinson's disease: substantia nigra regional selectivity. *Brain.* 1991;114:2283–2301.
9. Morrish PK, Rakshi JS, Bailey DL, Sawle GV, Brooks DJ. Measuring the rate of progression and estimating the preclinical period of Parkinson's disease with [^{18}F]dopa PET. *J Neurol Neurosurg Psychiatry.* 1998;64:314–319.
10. Bezard E, Dovero S, Prunier C, et al. Relationship between the appearance of symptoms and the level of nigrostriatal degeneration in a progressive 1-methyl-4-phenyl-1, 2, 3, 6-tetrahydropyridine-lesioned macaque model of Parkinson's disease. *J Neurosci.* 2001;21:6853–6861.
11. Ouchi Y, Nobezawa S, Okada H, Yoshikawa E, Futatsubashi M, Kaneko M. Altered glucose metabolism in the hippocampal head in memory impairment. *Neurology.* 1998;51:136–142.
12. Ouchi Y, Yoshikawa E, Sekine Y, et al. Microglial activation and dopamine terminal loss in early Parkinson's disease. *Ann Neurol.* 2005;57:168–175.
13. Mai J, Assheuer J, Paxinos G. *Atlas of the Human Brain.* New York, NY: Academic Press; 1997.
14. Ouchi Y, Okada H, Yoshikawa E, Nobezawa S, Futatsubash M. Brain activation during maintenance of standing postures in humans. *Brain.* 1999; 122:329–338.
15. Watanabe M, Shimizu K, Omura T, et al. A new high-resolution PET scanner dedicated to brain research. *IEEE Trans Nucl Sci.* 2002;49:634–639.
16. Rinne J, Sahlberg N, Ruottinen H, Nagren K, Lehikoinen P. Striatal uptake of the dopamine reuptake ligand [^{11}C] beta-CFT is reduced in Alzheimer's disease assessed by positron emission tomography. *Neurology.* 1998;50: 152–156.
17. Hughes AJ, Daniel SE, Kilford L, Lees AJ. Accuracy of clinical diagnosis of idiopathic Parkinson's disease: a clinico-pathological study of 100 cases. *J Neurol Neurosurg Psychiatry.* 1992;55:181–184.
18. Rajput AH, Rozdilsky B, Rajput A. Accuracy of clinical diagnosis in parkinsonism: a prospective study. *Can J Neurol Sci.* 1991;18:275–278.
19. Jankovic J, Rajput AH, McDermott MP, Perl DP. The evolution of diagnosis in early Parkinson disease. *Arch Neurol.* 2000;57:369–372.
20. Marek K, Jennings D, Tamagnan G, Seibyl J. Biomarkers for Parkinson's disease: tools to assess Parkinson's disease onset and progression. *Ann Neurol.* 2008;64:S111–S121.
21. Rinne OJ, Nurmi E, Ruottinen HM, Bergman J, Eskola O, Solin O. [^{18}F] FDOPA and [^{18}F] CFT are both sensitive PET markers to detect presynaptic dopaminergic hypofunction in early Parkinson's disease. *Synapse.* 2001;40:193–200.
22. Wong DF, Yung B, Dannals RF, et al. In vivo imaging of baboon and human dopamine transporters by positron emission tomography using [^{11}C]WIN 35,428. *Synapse.* 1993;15:130–142.
23. Hantraye P, Brownell AL, Elmaleh D, et al. Dopamine fiber detection by [^{11}C]-CFT and PET in a primate model of parkinsonism. *Neuroreport.* 1992;3:265–268.
24. Nirenberg MJ, Vaughan RA, Uhl GR, Kuhar MJ, Pickel VM. The dopamine transporter is localized to dendritic and axonal plasma membranes of nigrostriatal dopaminergic neurons. *J Neurosci.* 1996;16:436–447.
25. Mozley PD, Schneider JS, Acton PD, et al. Binding of [^{99m}Tc] TRODAT-1 to dopamine transporters in patients with Parkinson's disease and in healthy volunteers. *J Nucl Med.* 2000;41:584–589.

26. Nandhagopal R, Kuramoto L, Schulzer M, et al. Longitudinal progression of sporadic Parkinson's disease: a multi-tracer positron emission tomography study. *Brain.* 2009;132:2970–2979.
27. Martin WR, Wieler M, Stoessl A, Schulzer M. Dihydrotetrabenazine positron emission tomography imaging in early, untreated Parkinson's disease. *Ann Neurol.* 2008;63:388–394.
28. Szabo J. Organization of the ascending striatal afferents in monkeys. *J Comp Neurol.* 1980;189:307–321.
29. Benamer HTS, Patterson J, Wyper DJ, Hadley DM, Macphee GJA, Grosset DG. Correlation of Parkinson's disease severity and duration with ^{123}I-FP-CIT SPECT striatal uptake. *Mov Disord.* 2000;15:692–698.
30. Braak H, Del Tredici K, Rub U, de Vos RA, Jansen Steur EN, Braak E. Staging of brain pathology related to sporadic Parkinson's disease. *Neurobiol Aging.* 2003;24:197–211.
31. Lees AJ, Hardy J, Revesz T. Parkinson's disease. *Lancet.* 2009;373:2055–2066.
32. Marek KL, Seibyl JP, Zoghbi SS, et al. [^{123}I] beta-CIT/SPECT imaging demonstrates bilateral loss of dopamine transporters in hemi-Parkinson's disease. *Neurology.* 1996;46:231–237.
33. Lieberman A. Depression in Parkinson's disease: a review. *Acta Neurol Scand.* 2006;113:1–8.
34. Wise RA. Roles for nigrostriatal-not just mesocorticolimbic-dopamine in reward and addiction. *Trends Neurosci.* 2009;32:517–524.
35. Ito H Takahashi H, Arakawa R, Takano H, Suhara T. Normal database of dopaminergic neurotransmission system in human brain measured by positron emission tomography. *Neuroimage.* 2008;39:555–565.
36. Vingerhoets FJ, Schulzer M, Calne D, Snow B. Which clinical sign of Parkinson's disease best reflects the nigrostriatal lesion? *Ann Neurol.* 1997;41:58–64.
37. Pahwa R, Factor SA, Lyons KE, et al. Quality Standards Subcommittee of the American Academy of Neurology. Practice parameter: treatment of Parkinson disease with motor fluctuations and dyskinesia (an evidence-based review)—report of the Quality Standards Subcommittee of the American Academy of Neurology. *Neurology.* 2006;66:983–995.
38. Jubault T, Monetta L, Straffella AP, et al. L-dopa medication in Parkinson's disease restores activity in the motor cortico-striatal loop but does not modify the cognitive network. *PLoS ONE.* 2009;4:e6154.
39. Parkinson Study Group. Dopamine transporter brain imaging to assess the effects of pramipexole vs levodopa on Parkinson disease progression. *JAMA.* 2002;287:1653–1661.
40. Ravina B, Eidelberg D, Ahlskog JE, et al. The role of radiotracer imaging in Parkinson disease. *Neurology.* 2005;64:208–215.

Psychiatry and Clinical Neurosciences 2010; 64: 293–298 doi:10.1111/j.1440-1819.2010.02083.x

Regular Article

Frontal hypoperfusion in depressed patients with dementia of Alzheimer type demonstrated on 3DSRT

Kouhei Kataoka, MD,[1] Hiroshi Hashimoto, MD, PhD,[1]* Joji Kawabe, MD, PhD,[2] Shigeaki Higashiyama, MD, PhD,[2] Hisanori Akiyama, MD, PhD,[1] Aiko Shimada, MD,[1] Toshihiro Kai, MD, PhD,[3] Koki Inoue, MD, PhD,[1] Susumu Shiomi, MD, PhD[2] and Nobuo Kiriike, MD, PhD[1]

[1]*Department of Neuropsychiatry and* [2]*Nuclear Medicine, Osaka City University, Graduate School of Medicine and* [3]*Osaka City General Hospital, Osaka, Japan*

Aims: Depressive symptoms are common in patients with dementia of Alzheimer type (DAT) and contribute to clinical morbidity. Previous studies have suggested that hypoperfusion in the prefrontal cortex and anterior cingulate gyrus are involved in the pathophysiology of depression in DAT. Using 3-D stereotactic region of interest (ROI) template (3DSRT), fully automated ROI analysis software, the purpose of the present study was to investigate the relationship between depressive symptoms and regional cerebral blood flow (rCBF) in DAT.

Methods: Technetium-99*m*-ethyl cysteinate dimer (^{99m}Tc-ECD) single-photon emission computed tomography (SPECT) and Japanese version of the Neuropsychiatric Inventory (NPI) were carried out in 35 patients diagnosed as having mild–moderate DAT according to DSM-IV. These patients were divided into the depressive group (D group: $n = 17$) and non-depressive group (ND group: $n = 18$) using the NPI depression items. All data from SPECT images were analyzed using 3DSRT software. On 3DSRT the perfusion ratios (rCBF of bilateral callosomarginal, precentral, central, parietal, angular, temporal, posterior cerebral, pericallosal, lenticular nucleus, thalamus and hippocampus/cerebellar hemisphere) of each segment were compared between the D group and the ND group.

Results: The perfusion ratios of the left callosomarginal segment for the D group were significantly lower ($P < 0.05$) than those of the ND group.

Conclusions: Hypoperfusion in the left frontal cortex contributes to the expression of depressive symptoms in patients with DAT.

Key words: dementia, dementia of Alzheimer type, depression, single-photon emission computed tomography, 3-D stereotactic region of interest template.

DEPRESSIVE SYMPTOMS ARE common in patients with dementia of Alzheimer type[1] and it is often difficult to evaluate these symptoms in this patient population.

Although the etiology and pathologic mechanisms of depression in patients with DAT remain unclear, it would be clinically useful to develop a biological index that objectively evaluates depressive symptoms.

In a previous study we examined the relationship between depressive symptoms and regional cerebral blood flow (rCBF) in only two regions of interest (ROI): prefrontal cortex and anterior cingulate gyrus, on each side in patients with DAT, using a statistical image analysis program (easy Z-score imaging system: eZIS),[2] and reported the relationship between depressive symptoms and hypoperfusion in the left prefrontal cortex.[3] The study, however, could have lacked accuracy because of visual positioning of ROI

Correspondence: Hiroshi Hashimoto, MD, PhD, Department of Neuropsychiatry, Osaka City University, Graduate School of Medicine, 1-4-3, Asahi-machi, Abeno-ku, Osaka 545-8585, Japan. Email: hashimotoh@med.osaka-cu.ac.jp

Received 25 August 2009; revised 30 January 2010; accepted 6 February 2010.

and dispersions to evaluate hypoperfusion among observers.

In the current study, to confirm the previous findings, we investigated the relationship between depressive symptoms and rCBF of all brain domains in DAT patients using single-photon emission computed tomography (SPECT), Japanese version of the Neuropsychiatric Inventory (NPI)[4,5] and 3-D stereotactic ROI template (3DSRT).[6]

METHODS

Patients

Thirty-five right-handed patients (10 men, 25 women) diagnosed as having mild–moderate DAT were recruited from an outpatient clinic of the Department of Neuropsychiatry in Osaka City University Hospital. The mean patient age was 73.7 years and the mean duration of dementia was 1.7 years. Clinical diagnosis of DAT was based on the DSM-IV. Other causes of dementia were excluded by laboratory investigations, including magnetic resonance (MR) or computed tomography (CT) of the brain, thyroid function, venereal disease research laboratory (VDRL) test, Vitamin B_{12} and folate. None of the subjects was receiving medication to improve depressive symptoms or a cholinesterase inhibitor. The Institutional Review Board of the Osaka City University Hospital approved this study protocol, and informed consent was obtained from each patient and his or her family representative after a detailed explanation of the study.

Functional and behavioral assessment

Each participant has received clinical assessments before the SPECT imaging procedure. In order to assess the presence of cognitive function, the Revised Hasegawa Dementia Scale (HDS-R: score 0–30, with 0 being the most severe)[7] was used to screen all subjects with DAT. The HDS-R has been used exclusively in East Asian countries as a screening test for DAT. The optimal cut-off scores of the HDS-R for mild DAT are 20/21 in Japan. The global severity of dementia was determined according to the Clinical Dementia Rating (CDR).[8] Severe DAT patients having CDR = 3 were excluded in the present study.

Depressive symptoms were assessed with the NPI subscale for depression/dysphoria. The NPI has the advantages of evaluating a wider range of psychopathology than existing instruments, soliciting information that may distinguish among different etiologies of dementia, differentiating between severity and frequency of behavioral changes, and minimizing administration time.[4] We adopted the NPI to investigate the involvement of behavioral and psychological symptoms of dementia (BPSD) apart from depressive symptoms to rCBF. Caregivers were interviewed following the NPI procedures previously described; screening questions for each behavior were posed first. The caregiver was asked if the behavior represented a change from that exhibited by the patient prior to the onset of dementia and whether the behavior had been present during the previous month. If a positive response was obtained on the screening questions, then the behavioral domain was explored with scripted questions that focused on specific features of the behavioral disturbances. These behavioral domains consist of hallucination, delusion, agitation, depression/dysphoria, anxiety, euphoria, apathy, disinhibition, irritability and aberrant motor activity. The caregiver then rated the extent of the severity of the symptom: scores from 1 to 4 (with 4 being the most severe) for the frequency and from 1 to 3 (with 3 being the most severe) for the severity of each behavior. The composite score for each domain was the product of the frequency and severity subscores; the maximum attainable score was 12. The NPI has demonstrated content validity, convergent validity, item independence, interrater reliability and test–retest reliability in patients with DAT.[4,5] In the present study the 35 patients were divided into two groups: those with depressive symptoms (depressive group; caregiver confirmed patient depression on the NPI: D group: $n = 17$, five men, 12 women) and those without depressive symptoms (non-depressive [ND] group: $n = 18$, five men, 13 women).

Image acquisition and analysis

Each patient underwent brain perfusion SPECT with technetium-99*m*-ethyl cysteinate dimer (^{99m}Tc-ECD). For brain perfusion SPECT, an i.v. bolus of 740 MBq ^{99m}Tc-ECD was injected over a few seconds. During the 10-min uptake phase the patient rested in a dimly lit room with eyes closed and ears unplugged. Passage of the tracer from the aortic arch to the brain was monitored in a 128×128 matrix format for 120 s at 1-s intervals with a photo peak centered on 141 keV. The data

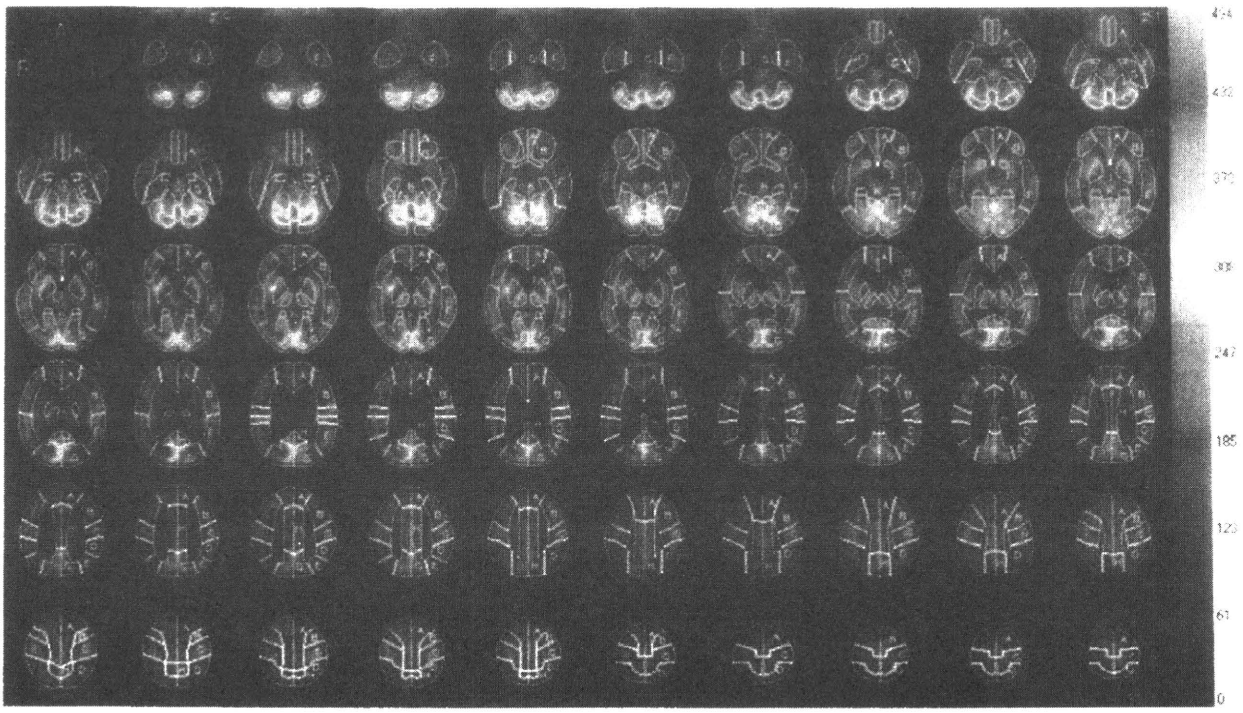

Figure 1. Brain perfusion single-photon emission computed tomography (SPECT) of a representative case. 3-D stereotactic region of interest (ROI) template (3DSRT) images with ROI delineation are shown on the ^{99m}Tc-ECD template. The segments are defined as follows: (A) callosomarginal, (B) precentral, (C) central, (D) parietal, (E) angular, (F) temporal, (G) posterior cerebral, (H) pericallosal, (I) lenticular nucleus, (J) thalamus, (K) hippocampus, (L) cerebellum segment. The inferior right to superior left sections correspond to the cranial–caudal horizontal sections in the subject. The left side corresponds to the right side of the horizontal sections in the subject.

were used for mean calculation of mean global CBF. Then, the SPECT projection data were acquired once for 20 min starting 5 min after i.v. injection of ^{99m}Tc-ECD with a triple-head rotating gamma camera and fanbeam high-resolution collimators (GCA9300; Toshiba, Tochigi, Japan). The photo peak was centered on 141 keV in 90 projections with 360° rotation (128 × 128 matrix format). Each scan was performed to obtain transverse images.[9] To confirm diagnosis of DAT, each SPECT image was analyzed using eZIS[2] before 3DSRT analysis.

3DSRT image analysis is a fully automated rCBF quantification computer program with an anatomical standardization engine transplanted from SPM2 and was carried out on a personal computer equipped with a Windows XP operating system. This program automatically measures the rCBF of 636 ROI, grouped into 12 paired segments, and covers almost the whole cerebral gray matter in only a few minutes.[6] The segments are defined as follows: callosomarginal, precentral, central, parietal, angular, temporal, posterior cerebral, pericallosal, lenticular nucleus, thalamus, hippocampus, and cerebellum segment (Fig. 1). The mean blood flow through each segment was automatically calculated with this program. In the present study we used the cerebellum as a reference region because that region has been used to normalize SPECT counts.[10,11] We calculated the perfusion ratios (rCBF of bilateral segments/cerebellar hemisphere) in each segment (callosomarginal, precentral, central, parietal, angular, temporal, posterior cerebral, pericallosal, lenticular nucleus, thalamus and hippocampus) to analyze individual rCBF semiquantitatively and compared the ratios between the D group and the ND group.

Statistical analysis

Statistical analysis was performed with SPSS for Windows 16.0 (SPSS Japan, Tokyo, Japan). We com-

Table 1. Patient characteristics vs presence of depression (mean ± SD)

	Depression group (n = 17)	Non-depression group (n = 18)	Total (n = 35)
Age, years	73.3 ± 7.3	73.4 ± 5.7	73.3 ± 6.5
Onset, years	72.1 ± 7.4	71.4 ± 5.7	71.8 ± 6.5
Duration of dementia, years	1.5 ± 1.3	1.9 ± 1.9	1.7 ± 1.6
Education, years	9.4 ± 2.2	10.0 ± 2.4	9.7 ± 2.3
HDS-R	16.5 ± 5.0	17.1 ± 7.9	16.8 ± 6.6
CDR	1.4 ± 0.5	1.2 ± 0.6	1.3 ± 0.6
NPI			
Depression item score	3.59 ± 2.80	0	1.88 ± 2.69
Anxiety item score	2.23 ± 3.14	1.67 ± 3.22	2.06 ± 3.15
Apathy item score	2.41 ± 2.79	1.64 ± 3.41	2.93 ± 3.43
NPI total score	20.4 ± 17.0	10.5 ± 7.3	15.8 ± 14.2

CDR, Clinical Dementia Rating; HDS-R, Revised Hasegawa Dementia Scale; NPI, Neuropsychiatric Inventory.

pared clinical characteristics between the D group and the ND group using two-sample t-test (Table 1). Categorical variables, such as sex, were compared on χ^2 test. We used repeated-measures analysis of variance (ANOVA) to compare the perfusion ratios in the D group and the ND group. The significance of the differences in the perfusion ratios for each segment between two groups was evaluated on Student's t-test for independent groups. All statistical tests were two-tailed and reported at $P < 0.05$.

RESULTS

All patients had significant rCBF reduction in the posterior cingulate gyrus and/or precuneus region on the SPECT images using eZIS.

No significant differences were observed between the D and the ND groups with respect to patient age, age at onset of the disease, duration of DAT/dementia, years of education, HDS-R score, CDR, NPI total score, NPI anxiety and apathy item scores (Table 1). In addition, on χ^2 analysis there was also no significant difference between the groups with regard to sex and family history of dementia.

Repeated-measures ANOVA indicated a significant main effect of group with regard to D versus ND group ($F(1,21) = 57.395$, $P < 0.001$). The D group had a significant decrease of the perfusion ratio in the left callosomarginal segment compared with the ND group ($P < 0.05$). There were no significant differences between the two groups in the ratios in the right hemisphere, but there was a tendency toward lower perfusion in the right callosomarginal segment in the D group ($P = 0.05$; Table 2).

DISCUSSION

The current study suggests that hypoperfusion in the left callosomarginal region in patients with DAT is related to depressive symptoms assessed on the NPI. This region contains the left prefrontal cortex, which in our previous study using eZIS, was suggested to be related to depressive symptoms in patients with DAT. Furthermore, there was no relationship between depressive symptoms and rCBF in other regions. Therefore, the present study again suggests a relationship between depressive symptoms in DAT and hypoperfusion in the frontal cortex. On 3DSRT the callosomarginal segment consisted of the superior frontal, medial frontal, paracentral lobule, anterior cingulate, subcallosal, orbital, and rectal subsegments. Therefore, it is necessary to perform further research to clarify the region most related to depressive symptoms in DAT.

In our previous study we were not able to investigate the relationship between other brain regions and depressive symptoms in patients with DAT because we focused only on the prefrontal cortex and anterior cingulate gyrus,[3] which have been reported to be associated with primary depression.[12] Furthermore, eZIS showed interobserver differences in the evaluation of hypoperfusion and inaccuracies with the positioning of the ROI because more than one observer visually assessed hypoperfusion in these regions. In the present study, 3DSRT removed these problems by allowing automatic ROI analysis of the brain with high objectivity and excellent reproducibility. Therefore, in the present study we applied 3DSRT in order to confirm the reliability of our previous study with eZIS.

Table 2. Perfusion ratios (rCBF of bilateral segments/cerebellar hemisphere) vs presence of depression

	D group		ND group		D vs ND group		
Segment	Mean	SD	Mean	SD	*t*	d.f.	*P*
Callosomarginal right	0.729	0.080	0.773	0.080	1.980	33	0.05
Callosomarginal left	0.690	0.084	0.748	0.081	2.073	33	0.05*
Precentral right	0.759	0.070	0.795	0.083	1.356	33	0.18
Precentral left	0.710	0.075	0.760	0.082	1.888	33	0.07
Central right	0.699	0.076	0.725	0.076	0.990	33	0.32
Central left	0.698	0.069	0.722	0.080	0.095	33	0.35
Parietal right	0.642	0.073	0.650	0.092	0.283	33	0.78
Parietal left	0.619	0.076	0.656	0.097	1.239	33	0.22
Angular right	0.704	0.076	0.707	0.096	0.077	33	0.94
Angular left	0.670	0.087	0.727	0.101	0.963	33	0.34
Temporal right	0.708	0.067	0.690	0.076	−0.717	33	0.49
Temporal left	0.670	0.083	0.688	0.090	0.619	33	0.54
Posterior cerebral right	0.817	0.060	0.796	0.054	−1.073	33	0.29
Posterior cerebral left	0.796	0.069	0.796	0.083	0.021	33	0.98
Pericallosal right	0.719	0.066	0.742	0.061	1.099	33	0.28
Pericallosal left	0.691	0.072	0.725	0.086	1.277	33	0.21
Lenticular nucleus right	0.853	0.092	0.866	0.058	0.490	33	0.63
Lenticular nucleus left	0.829	0.086	0.835	0.074	0.207	33	0.84
Thalamus right	0.749	0.085	0.769	0.097	0.653	33	0.52
Thalamus left	0.741	0.086	0.786	0.105	1.356	33	0.18
Hippocampus right	0.618	0.060	0.610	0.053	−0.404	33	0.69
Hippocampus left	0.582	0.081	0.596	0.083	0.475	33	0.64

*$P < 0.05$.

D group, patients with depressive symptoms; ND group, patients without depressive symptoms; rCBF, regional cerebral blood flow.

The association between depressive symptoms and rCBF in patients with DAT has been investigated in several SPECT studies.[3,11,13–15] Most SPECT studies have demonstrated an association between depressive symptoms and hypoperfusion in the prefrontal cortex[11] or anterior cingulate gyrus.[13] In contrast, recent positron emission tomography studies have also indicated that frontal dysfunction is associated with depressive symptoms in patients with DAT.[14,15] The present results are consistent with previous neuroimaging studies suggesting that frontal dysfunction is associated with the expression of depressive symptoms in patients with DAT. Previous findings on brain lateralization in depressive patients with DAT, however, have been conflicting.[3,11,13,14] The present findings demonstrated that the left frontal cortex is significantly related to depressive symptoms in DAT. In contrast, Levy-Cooperman *et al.* reported that the right hemisphere is strongly associated with these symptoms.[11] Laterality effects might be caused by several factors, such as the influence of other lesions or the severity of the disease, or may reflect sample size and statistical thresholds. Although the finding had lower significance, the present study also demonstrated hypoperfusion in the right callosomarginal region in depressed patients with DAT ($P = 0.05$). More detailed assessment of lateralization should be explored in further studies.

Frontal dysfunction has been reported in functional image studies in primary depression[12] and secondary depression due to other disease such as Parkinson's disease[16] and Huntington's disease.[17] Although the cause of frontal dysfunction in these patients remains unclear, the present results are consistent with these findings that this region is related to expression of depressive symptoms, regardless of the underlying disease.

There are some limitations to the present study. The first is the problem of the method of semiquantifying rCBF in 3DSRT. In most SPECT studies of DAT, cerebellar perfusion has been used as a reference region

because it is less involved in the progression of DAT.[10,11,18] There is a report, however, that cerebellar glucose metabolism was significantly reduced in advanced Alzheimer's disease,[19] and cerebellar perfusion could also be lower in the severe state. Therefore, we excluded subjects with CDR = 3 to minimize this effect and we will examine this issue further using the primary visual region as a reference region, because that area is much less involved in the disease. Second, we must consider the presence of BPSD apart from depressive symptoms, which may influence rCBF. In the current study there was no significant difference in the NPI anxiety and apathy item scores between the two groups, but we need a further investigation because the NPI total score tended to be higher in the D group. Third, the analyses do not consider interactions with rCBF or atrophy in other brain areas. It is also possible that anatomically distant lesions contribute to depressive symptoms through the neural network. Fourth, we used DSM-IV to diagnose presence of DAT and did not carry out neuropsychological assessment except for the HDS-R. We need further research to raise the accuracy of DAT diagnosis by using neuropsychological test. Finally, the mechanism of the relationship between rCBF in the frontal lobe and depressive symptoms in patients with DAT is unclear. Further studies are needed to develop the current findings into practical applications for treating patients with DAT.

ACKNOWLEDGMENT

This study was supported by the Medical Research Foundation for Senile Dementia of Osaka.

REFERENCES

1. Vilalta-Franch J, Garre-Olmo J, Lopez-Pousa S *et al.* Comparison of different clinical diagnostic criteria for depression in Alzheimer disease. *Am. J. Geriatr. Psychiatry* 2006; 14: 589–597.
2. Mizumura S, Kumita S. Stereotactic statistical imaging analysis of the brain using the easy Z-score imaging system for sharing a normal database. *Radiat. Med.* 2006; 24: 545–552.
3. Akiyama H, Hashimoto H, Kawabe J *et al.* The relationship between depressive symptoms and prefrontal hypoperfusion demonstrated by eZIS in patients with DAT. *Neurosci. Lett.* 2008; 441: 328–331.
4. Cummings JL, Mega M, Gray K, Rosenberg-Thompson S, Carusi DA, Gornbein J. The Neuropsychiatric Inventory: Comprehensive assessment of psychopathology in dementia. *Neurology* 1994; 44: 2308–2314.
5. Hirono N, Mori E, Ikejiri Y *et al.* [Japanese version of the Neuropsychiatric Inventory: A scoring system for neuropsychiatric disturbances in dementia patients]. *No To Shinkei* 1997; 49: 266–271.
6. Takeuchi R, Sengoku T, Matsumura K. Usefulness of fully automated constant ROI analysis software for the brain: 3DSRT and FineSRT. *Radiat. Med.* 2006; 24: 538–544.
7. Kim KW, Lee DY, Jhoo JH *et al.* Diagnostic accuracy of mini-mental status examination and revised Hasegawa dementia scale for Alzheimer's disease. *Dement. Geriatr. Cogn. Disord.* 2005; 19: 324–330.
8. Berg L. Clinical Dementia Rating (CDR). *Psychopharmacol. Bull.* 1988; 24: 637–639.
9. Higashiyama S, Kawabe J, Hashimoto H *et al.* 3DSRT evaluation of responses of Alzheimer type dementia to donepezil hydrochloride therapy. *Osaka City Med. J.* 2006; 52: 55–62.
10. Pickut BA, Dierckx RA, Dobbeleir A *et al.* Validation of the cerebellum as a reference region for SPECT quantification in patients suffering from dementia of the Alzheimer type. *Psychiatry Res.* 1999; 90: 103–112.
11. Levy-Cooperman N, Burhan AM, Rafi-Tari S *et al.* Frontal lobe hypoperfusion and depressive symptoms in Alzheimer disease. *J. Psychiatry Neurosci.* 2008; 33: 218–226.
12. Ito H, Kawashima R, Awata S *et al.* Hypoperfusion in the limbic system and prefrontal cortex in depression: SPECT with anatomic standardization technique. *J. Nucl. Med.* 1996; 37: 410–414.
13. Liao YC, Liu RS, Lee YC *et al.* Selective hypoperfusion of anterior cingulate gyrus in depressed AD patients: A brain SPECT finding by statistical parametric mapping. *Dement. Geriatr. Cogn. Disord.* 2003; 16: 238–244.
14. Lee DY, Choo IH, Jhoo JH *et al.* Frontal dysfunction underlies depressive syndrome in Alzheimer disease: A FDG-PET study. *Am. J. Geriatr. Psychiatry* 2006; 14: 625–628.
15. Holthoff VA, Beuthien-Baumann B, Kalbe E *et al.* Regional cerebral metabolism in early Alzheimer's disease with clinically significant apathy or depression. *Biol. Psychiatry* 2005; 57: 412–421.
16. Mayberg HS, Starkstein SE, Sadzot B *et al.* Selective hypometabolism in the inferior frontal lobe in depressed patients with Parkinson's disease. *Ann. Neurol.* 1990; 28: 57–64.
17. Mayberg HS, Starkstein SE, Peyser CE, Brandt J, Dannals RF, Folstein SE. Paralimbic frontal lobe hypometabolism in depression associated with Huntington's disease. *Neurology* 1992; 42: 1791–1797.
18. Kobayashi S, Tateno M, Utsumi K *et al.* Quantitative analysis of brain perfusion SPECT in Alzheimer's disease using a fully automated regional cerebral blood flow quantification software, 3DSRT. *J. Neurol. Sci.* 2008; 264: 27–33.
19. Ishii K, Sasaki M, Kitagaki H *et al.* Reduction of cerebellar glucose metabolism in advanced Alzheimer's disease. *J. Nucl. Med.* 1997; 38: 925–928.

EDITORIAL

Emerging in vivo evidence of subcortical cholinergic dysfunction in parkinsonian syndromes

Hitoshi Shinotoh, MD, PhD
Shigeki Hirano, MD, PhD

Address correspondence and reprint requests to Dr. H. Shinotoh, Molecular Neuroimaging Group, Molecular Imaging Center, National Institute of Radiological Sciences, 4-9-1 Anagawa, Inage-ku, Chiba-shi, Chiba 263-8555, Japan
hitoshi.shinoto@nifty.com

Neurology® 2010;74:1406–1407

Development of CNS imaging using the radioactive acetylcholine analog method in the mid-1990s opened a window on cerebral cholinergic function in vivo.[1] Two PET tracers, [^{11}C]MP4A and its sister compound [^{11}C]PMP (or [^{11}C]MP4P), are currently used in vivo for measurement of brain acetylcholinesterase (AChE) activity in humans. Both radiotracers readily pass through the blood–brain barrier following IV injection and are hydrolyzed by AChE localized within the intersynaptic space, predominantly on presynaptic cholinergic neurons. Subsequently, radiolabeled metabolites are trapped locally in the brain according to the distribution of enzyme activity.

PET studies using these radiotracers have revealed reduction of cerebral cortical AChE activity in Alzheimer disease (AD)[2] and Parkinson disease (PD),[3,4] as well as more severe reduction of cortical AChE activity in PD with dementia (PDD)[4] and dementia with Lewy bodies (DLB),[4] which suggests loss of ascending cholinergic projections from the basal forebrain. Reduction of cortical AChE activity is correlated in turn with cognitive dysfunction in AD,[2] PD, and PDD/DLB,[4] indicating that the loss of the ascending cholinergic system from the basal forebrain plays a pivotal role in cognitive dysfunction in these disorders. A recent PET study showed that patients with PD who had falls showed a greater reduction of AChE activity in the thalamus and the cerebral cortex than patients with PD without falls.[5] The pedunculopontine nucleus (PPN), a brainstem locomotor center, and the laterodorsal tegmental nucleus (LDT) provide cholinergic projections to the thalamus, basal ganglia, cerebellum, and the pontine and medullary reticular formation. Therefore, the more severe reduction of thalamic AChE activities in PD fallers than nonfallers was interpreted as a more severe loss of ascending cholinergic projections from PPN and LDT in PD fallers, indicating that PPN degeneration is a major factor in the development of impaired control and gait dysfunction in PD. In progressive supranuclear palsy (PSP), PET studies showed a prominent loss of thalamic AChE activity with relative preservation of cerebral cortical AChE activity.[3] In patients with the cerebellar variant of multiple system atrophy (MSA-C) and spinocerebellar ataxia type-3 (SCA-3), PET studies showed loss of thalamic AChE activity with normal cerebral cortical AChE activity.[6] Thalamic AChE activities of SCA-3 patients were inversely correlated with the Unified Parkinson's Disease Rating Scale motor subscore.[6]

AChE activities differ grossly across different brain cholinergic structures, with cerebral cortex/cerebellar hemisphere/caudate enzyme activities having relative values of 1.0/12.0/54.7, as determined in normal brain at postmortem.[7] Estimation in brain regions with high AChE activity in vivo, such as the brainstem, cerebellum, and striatum, is more challenging in PET studies using these radiotracers because of the ceiling effect, in which flow-limited delivery of tracers can underestimate the highest activities.[8] Therefore, there has been only one in vivo study on alteration of AChE activity in the cerebellum and striatum in neurologic disorders.[6]

In this issue of *Neurology*®, Gilman et al.[9] report an elegant PET study that avoids the ceiling effect by use of a refined technique using stabilizing kinetic analysis of [^{11}C]PMP.[8,9] This study shows cholinergic denervation of cerebral cortical and subcortical regions in PD, and the parkinsonian syndromes of MSA (MSA-P) and PSP. They found that AChE activity was significantly decreased in the cerebral cortical regions in 12 patients with PD (−15.4%) and 13 MSA-P patients (−14.6%) with similar but nonsignificant declines seen in 4 PSP patients (−13.2%) compared with 22 normal controls. AChE activity was also decreased in the striatum (−19.5%), cerebellum (−22.9%), thalamus (−14.7%), and midbrain (−11.5%) in patients with PD, and further declines were seen in patients with MSA-P (−38.6%, −40.2%, −34.6%, −25.9%, respectively, in the above-mentioned regions) and patients with PSP (−41.3%, −24.1%, −17.6%, −20.0%) compared with normal controls. Interestingly, the severity of the balance and gait disorders in PD, MSA-P, and

See page 1416

From the Molecular Neuroimaging Group, Molecular Imaging Center, National Institute of Radiological Sciences, Japan.
Disclosure: The authors report no disclosures.

PSP were correlated with the reduction of AChE activity in the midbrain ($p < 0.025$) and cerebellum ($p < 0.013$), but not for any other region. The more substantial cholinergic decreases in MSA-P and PSP reflect greater involvement of the brainstem cholinergic group including PPN, which may account for the greater gait disturbances in the early stages of MSA-P and PSP than in PD. The interpretation of the present PET results is supported by previous postmortem brain studies showing a significant reduction of PPN neurons in PD, and more profound reductions in PSP and MSA.

There are reports of dramatic improvement of gait disorders following PPN electrical stimulation in PD, but the results of a recent double-blind study of PPN stimulation in PD were rather disappointing compared to the high expectations raised by previous open-label studies.[10] The dysfunction of the brain cholinergic system observed in the study by Gilman et al.[9] suggests that there may be a role for cholinergic modulating drugs in the treatment of PD, MSA, and PSP.

There is one potential limitation necessitating caution in interpreting the results of Gilman et al. Atrophy (partial volume) effect on AChE activity measurement is not negligible in this technique,[8] despite the fact that they placed regions of interest on the peak of activity in an anatomic region to avoid atrophy effect. AChE activities in brain regions with atrophy may be underestimated in this study because insufficient image resolution leads to a mixing of the gray matter, white matter, and CSF within regions of interest. Despite the potential confound, this is the first report demonstrating cholinergic deficits in the striatum and cerebellum in PD, PSP, and MSA-P; such results can point the way for additional studies, and, equally if not more important, therapeutic trials.

REFERENCES

1. Irie T, Fukushi K, Akimoto Y, et al. Design and evaluation of radioactive acetylcholine analogs for mapping brain acetylcholinesterase (AChE) in vivo. Nucl Med Biol 1994;21:801–808.
2. Shinotoh H, Namba H, Fukushi K, et al. Progressive loss of cortical acetylcholinesterase activity in association with cognitive decline in Alzheimer's disease: a positron emission tomography study. Ann Neurol 2000;48:194–200.
3. Shinotoh H, Namba H, Yamaguchi M, et. al. Positron emission tomographic measurement of acetylcholinesterase activity reveals differential loss of ascending cholinergic systems in Parkinson's disease and progressive supranuclear palsy. Ann Neurol 1999;46:62–69.
4. Bohnen NI, Kaufer DI, Ivanco LS, et al. Cortical cholinergic function is more severely affected in parkinsonian dementia than in Alzheimer disease: an in vivo positron emission tomographic study. Arch Neurol 2003;60:1745–1748.
5. Bohnen NI, Müller ML, Koeppe RA, et al. History of falls in Parkinson disease is associated with reduced cholinergic activity. Neurology 2009;73:1670–1676.
6. Hirano S, Shinotoh H, Arai K, et al. PET study of brain acetylcholinesterase in cerebellar degenerative disorders. Mov Disord 2008;23:1154–1160.
7. Atack JR, Perry EK, Bonham JR, et al. Molecular forms of acetylcholinesterase and butyrylcholinesterase in the aged human central nervous system. J Neurochem 1986;47:263–277.
8. Koeppe RA, Frey KA, Snyder SE, Meyer P, et al. Kinetic modeling of *N*-[^{11}C]methylpiperidin-4-yl propionate: alternatives for analysis of an irreversible positron emission tomography trace for measurement of acetylcholinesterase activity in human brain. J Cereb Blood Flow Metab 1999;19:1150–1163.
9. Gilman S, Koeppe RA, Nan B, et al. Cerebral cortical and subcortical cholinergic deficits in parkinsonian syndromes. Neurology 2010;74:1416–1423.
10. Ferraye MU, Debû B, Fraix V, et al. Effects of pedunculopontine nucleus area stimulation on gait disorders in Parkinson's disease. Brain 2010;133:205–214.

Early Detection and Rehabilitation Technologies for Dementia:

Neuroscience and Biomedical Applications

Jinglong Wu
Okayama University, Japan

Medical Information Science
REFERENCE

Senior Editorial Director:	Kristin Klinger
Director of Book Publications:	Julia Mosemann
Editorial Director:	Lindsay Johnston
Acquisitions Editor:	Erika Carter
Development Editor:	Myla Harty
Production Coordinator:	Jamie Snavely
Typesetters:	Mike Brehm, Jennifer Romanchak and Deanna Jo Zombro
Cover Design:	Nick Newcomer

Published in the United States of America by
Medical Information Science Reference (an imprint of IGI Global)
701 E. Chocolate Avenue
Hershey PA 17033
Tel: 717-533-8845
Fax: 717-533-8661
E-mail: cust@igi-global.com
Web site: http://www.igi-global.com/reference

Library of Congress Cataloging-in-Publication Data

Early detection and rehabilitation technologies for dementia: neuroscience and biomedical applications / Jinglong Wu, editor.
p. ; cm.
Includes bibliographical references and index.
Summary: "This book provides a comprehensive collection for experts in the Neuroscience and Biomedical technology fields, outlining various concepts from cognitive neuroscience and dementia to neural technology and rehabilitation"-- Provided by publisher.
ISBN 978-1-60960-559-9 (hardcover) -- ISBN 978-1-60960-560-5 (ebook) 1. Dementia--Diagnosis. 2. Neurologic examination. I. Wu, Jinglong, 1958-
[DNLM: 1. Dementia. 2. Brain--physiopathology. 3. Diagnostic Techniques, Neurological. 4. Early Diagnosis. WM 220]
RC521.E27 2011
616.8'3--dc22
2010054442

British Cataloguing in Publication Data
A Cataloguing in Publication record for this book is available from the British Library.

Chapter 29
Quantitative Analysis of Amyloid β Deposition in Patients with Alzheimer's Disease Using Positron Emission Tomography

Manabu Tashiro
Cyclotron Nuclear Medicine, Tohoku University, Japan

Nobuyuki Okamura
Department of Pharmacology, Tohoku University Graduate School of Medicine, Japan

Shoichi Watanuki
Cyclotron Nuclear Medicine, Tohoku University, Japan

Shozo Furumoto
Radiopharmaceutical Chemistry, Cyclotron and Radioisotope Center, Tohoku University, Japan & Department of Pharmacology, Tohoku University Graduate School of Medicine, Japan

Katsutoshi Furukawa
Department of Geriatrics and Gerontology, Institute of Development, Aging and Cancer, Tohoku University, Japan

Yoshihito Funaki
Radiopharmaceutical Chemistry, Cyclotron and Radioisotope Center, Tohoku University, Japan

Ren Iwata
Radiopharmaceutical Chemistry, Cyclotron and Radioisotope Center, Tohoku University, Japan

Yukitsuka Kudo
Innovation of New Biomedical Engineering Center, Tohoku University Hospital, Japan

Hiroyuki Arai
Department of Geriatrics and Gerontology, Institute of Development, Aging and Cancer, Tohoku University, Japan

Hiroshi Watabe
Department of Molecular Imaging in Medicine, Osaka University Graduate School of Medicine, Japan

Kazuhiko Yanai
Cyclotron Nuclear Medicine, Tohoku University, Japan & Radiopharmaceutical Chemistry, Cyclotron and Radioisotope Center, Tohoku University, Japan

DOI: 10.4018/978-1-60960-559-9.ch029